AN ABSTRACT OF THE THESIS OF

John Hunt for the degree of Master of Science in Chemical Engineering presented on September 21, 2004.

Title: The Testing and Repair of Polyethylene Natural Gas Distribution Pipe

Abstract approved:

Redacted for privacy

Skip Rochefort

With the dominance of polyethylene as the building material for America's natural gas distribution system and a growing demand for natural gas, there exists and ever increasing need for improved methods of repairing damaged natural gas distribution pipe. This paper serves as the ground work for a multi-part study seeking to address this need by working towards the development of a polyethylene pipe repair patch that can easily be applied to damaged sections of pipe with minimal labor.

The first part of the study addresses the stresses present in a section of natural gas pipe and the criteria demanded of a successful patch adhesive. Tensile testing techniques are used to evaluate potential adhesives and finite element modeling is used to determine the maximum expected stresses experienced by the patch on a section of polyethylene pipe.

The second part of the study addresses the need for the section of pipe to maintain its structural integrity after the application of the patch and goes into the testing required to validate polyethylene gas pipe that has been damaged and repaired using the polyethylene pipe repair patch.

# The Testing and Repair of Polyethylene Natural Gas Distribution Pipe

by

John Hunt

A THESIS

submitted to

Oregon State University

in partial fulfillment of

the requirements for the

degree of

Master of Science

Presented September 21, 2004

Commencement June 2005

Master of Science thesis of John Hunt presented on September 21, 2004

APPROVED

Redacted for privacy

Major Professor, representing Chemical Engineering

Redacted for privacy

Head of the Department of Chemical Engineering

Redacted for privacy

Dean of the Graduate School

I understand that my thesis will become part of the permanent collection of Oregon State University libraries. My signature below authorizes release of my thesis to any reader upon request.

Redacted for privacy

John Hunt, Author

## ACKNOWLEDGMENTS

I would like to give thanks to everyone who helped make this possible.

Katherine Knox, my wife for all her support.

Skip Rochefort, for taking me in and seeing me through to the end.

Joel Hartter, Amy Harvey, and Samantha Lewis for their held during the summer.

Kevin Harris and Nick Wannamacher for technical assistance and personal support.

Cheryl Carbone for her tensile test work.

Goran Jovonovich, Michael Schuyler, and Brian Wood for being on my committee.

My friends, family and the all the O.S.U. Chemical Engineering students, faculty and staff for being there for me.

# TABLE OF CONTENTS

# LIST OF FIGURES

# LIST OF TABLES

# 1.0 INTRODUCTION

The purpose of this project is two-fold: first, it is to describe the initial development of a repair patch capable of bonding with high density polyethylene (HDPE) natural gas distribution pipe; second, to develop a tool for validating the hydrostatic design basis (HDB) of a HDPE gas pipe that has been either crimped or patched. Both purposes are intimately tied to a two-part research project in collaboration with Timberline Tool funded by the Department of Energy through the Small Business Initiatives Research (SBIR) DE-FG02-03ER83858 and the National Energy Technology Laboratory (NETL) DE-FC26-03NT41879.

Chapter two of this work focuses on the development of a pipe repair patch, specifically the judging criteria of the effectiveness of an adhesive repair patch and experimental technique development. This initial work will open up the way either to develop an HDPE adhesive patch in house or to evaluate commercially available adhesives for use in a repair patch. Ultimately the HDPE adhesive patch chosen will be integrated into an innovative new pipe-repair tool in development by Timberline Tool Company.

Chapter three is dedicated to the criteria and initial modeling and design of a pipe burst apparatus for the validation of plastic pipe hydrostatic design basis. This apparatus will, in turn, be used to evaluate the effectiveness of another Timberline Tool Company product being developed to crimp MDPE natural gas distribution pipe. This sort of evaluation is necessary to ensure that the pipe, once crimped and released, still performs at its listed hydrostatic design basis. It will also be used to evaluate the quality of the pipe repair patches and applicator tools.

# 2.0 POLYETHYLENE ADHESIVE PATCH

## 2.01 BACKGROUND

### 2.01.A PURPOSE OF RESEARCH

The use of polyethylene (PE) pipe for natural gas transmission and distribution within the United States has been steadily growing over the past decade and currently accounts for a majority of America's natural gas distribution network. It is very important that the natural gas delivery system remain safe, reliable, and operate efficiently. The current delivery system consists of 650 thousand miles of underground plastic piping that has been in service for over 30 years. The AGA report, "Fueling the Future" (Laramie, P. 9/2001), predicts that natural gas consumption will grow as much as 50 percent over the next 20 years. The number of miles of distribution and transmission polyethylene (PE) pipe will increase to meet this demand. According to the Department of Energy reports (United States DOE/NETL 9/2002), a special need exists for improved tools for construction, maintenance, and repair of PE pipe to keep up with the expected growth.

### 2.01.B POLYETHYLENE BONDING

With the addition of many more services each year, it is critical to develop tools for safe, reliable, and cost-effective repair of damaged or defective polyethylene pipe. Although polyethylene is known for its strength, chemical and moisture resistance, ease of manufacture, and low cost, it also is also known for its low surface energy, making most adhesives ineffective for bonding PE, either to itself or to other materials (Brewis, et. al. 1993, 1995). To overcome this, most methods for

connecting joints and ends use heat-welding techniques--such as electro-fusion--when installing, maintaining, or repairing PE pipelines (Hess, R. 10/2003). These methods require a great deal of excavation to access the damaged pipe, extensive man-hours to complete the repairs, and pose potential safety risks to workers, thus leading to a demand for alternative repair methods.

There are currently several methods used for joining polyethylene commercially; most are used for the production of PE parts and only a few are used in the natural gas industry. Of those methods, several are purely mechanical or thermal in nature including: ultrasonic welding, friction welding, vibration welding, heated tool welding, hot gas welding, and implant welding (Watson, M.N. 1998). Of these, only two are used in the United States natural gas industry today, and then only for joining sections of pipe, not for repairing damaged surfaces. Heated tool welding, also known as hot plate welding, is commonly used for joining large diameter sections of pipe, while implant welding, more often called electro-fusion welding, is used to fuse small diameter sections of pipe. These methods are all related through the use of heat to melt and join plastic pieces, whether or not the heating source is mechanical (ultrasonic, friction, and vibration welding) or electrical (heated tool, hot gas, and implant welding) (Hess, R. 10/2003).

Some adhesive welding methods for PE also exist, but most of them require at least minimal surface treatment, whether the treatment is chemical (chromic acid), thermal, plasma based, etc. Recently though, there have been a few PE adhesives on the market specifically designed so that they do not require any surface pretreatment other than the cleaning of dirt and grease or perhaps light

sanding (Tech. Data Sheets: 3M DP8005, DP8010, Phillystran Socketfast Blue). These newer adhesives offer both high strength and resistance to environmental effects such as moisture and temperature along with ease of application. The only potential disadvantages stem from the amount of time it takes for the adhesive to cure, which directly relates to the amount of time an operator would be required to keep an excavation site open and hold the patch in place until the adhesive finishes curing.

## 2.01.C ADHESIVE PATCH APPLICATION

The proposed adhesive patch, regardless of adhesive method, is intended to be applied using a patch delivery tool currently under development by Timberline Tool Company. Using their tool, which utilized a patented parallel-jaw design, the patch will be delivered through a relatively small diameter (less than 14") "key-hole" opening to the damaged section of pipe. Presuming that prior to patch application the pipe has been adequately cleared of dirt, grease, and moisture, the tool will hold the patch in place long enough to allow the adhesive to cure to its working strength. If needed, the tool can be designed to provide controlled heating of the patch to facilitate curing. The specific cleaning, cure-time, and temperature requirements will depend entirely on the nature of the adhesive chosen. These criteria will be discussed more thoroughly later in this work.

## 2.01.D GOALS OF STUDY

Ultimately, the goals of this study are as follows:

1. Develop or find an adhesive patch that has a strong bonding affinity with high density polyethylene resulting in high mechanical strength.

2. Ideally the adhesive should not require extensive surface pretreatment outside of simple cleaning or sanding. Chemical and other similarly complicated surface treatments are to be avoided.
3. The patch must be easy to apply with a simple pipe repair tool.
4. The adhesive patch must be sufficiently strong such that the hydrostatic design basis of the repaired pipe is maintained.
5. The adhesive patch must be safe for operators to apply and have minimal environmental impact, as well as displaying good environmental resistance to moisture and temperature and a long working life.

As stated in section 1.0, this paper will focus on developing the judging criteria for evaluating whether or not an adhesive patch meets the goals stated above. This paper will also focus on developing the experimental methods used for evaluating the first set of adhesives tested. These methods should remain pertinent for future adhesive choices, except perhaps in the case of a polyethylene gel adhesive patch, in which case new methods may need to be investigated.

## 2.02 LITERATURE REVIEW

Adhesion between polymer surfaces--in particular the problems related to adhesion--is at the heart of developing a successful repair patch for polyethylene (PE) pipe. People have been using adhesives for over three thousand years, but an attempt to understand the nature of adhesion and the principles behind it was not attempted until recent times [Allen, K.W. 1993]. Of particular interest to this study are the reasons behind the poor adhesion properties generally noted in polyolefins (PE in particular) and methods of conforming to or improving those properties so that an adequate structural bond can be developed. The following section will overview papers that cover general theories of adhesion before moving on more specifically to polymer adhesion, and finally, the use of polymer gels as adhesives.

According to Allen [Allen, K.W. 1993], there are three general groups of forces that effect adhesion. The first are mechanical forces, these are the simplest to see and generally require nothing more than a strong rough surface to facilitate bonding. For example, Velcro cloth is an extreme case of adhesion due to mechanical forces, where adhesion is possible due to the interlinking of rough surfaces. The second group of forces is derived from weak intermolecular interactions such as van der Waals interactions. Van der Waals interactions require very close proximity (less than 10 Å) to take effect, which in turn require good wetting and spreading properties between the two surfaces to be adhered. Finally there are primary valence bonding forces such as covalent, ionic, and metallic bonds. This kind of adhesion only takes place when there is some sort of chemical reaction at the interface and typically represents the strongest type of adhesive bond

(Chung, F.H. 1991), though for polymer-polymer adhesion it is relatively rare (Jabbari, Peppas 1994). Hydrogen bonding can also be included as a primary valence force, though it is not as strong (11). Chung rates the ratios of bond forces between covalent/hydrogen/van der Waals forces as 1000/40/1 (11). Hydrogen bonding and van der Waals forces are the leading reasons for most non-mechanical adhesion, taking into account that covalent forces for adhesion are only available under special circumstances.

Jabbari and Peppas take a detailed look at polymer adhesion, proposing three primary theories for polymer-polymer inter-diffusion and adhesion (Jabbari, Peppas 1994). They assume that most polymer-polymer adhesion occurs between non-porous surfaces that do not display "chemical-healing" properties (i.e. no chemical reactions occur at the interface). They propose that wetting, fracture and diffusion theories of adhesion most accurately describe what happens in the case of polymer surfaces.

Wetting theory concerns the wetting of one polymer surface onto another surface and is strongly influenced by the surface and interfacial free energies of the polymers involved. The spreading coefficient, S, is defined as:

$$S = \Gamma_1 - \Gamma_2 - \Gamma_{12} \qquad \text{Equation 2.01.1}$$

Where $\Gamma_1$and $\Gamma_2$ are the surface free energies of the two polymers and $\Gamma_{12}$ is the interfacial free energy between the two polymers. Good wetting occurs when $S > 0$ and poor wetting occurs when $S < 0$. Two things are able to happen when the polymer surfaces experience good wetting (Jabbari, Peppas 1994). One, van der Waals interactions are possible between the two surfaces (Allen, 1993) and secondly the

polymer interface disappears and polymer chains are free to inter-diffuse (Jabbari, Peppas 1994).

Diffusion theory addresses the inter-diffusion of polymer chains between two polymer surfaces. Once two surfaces have undergone perfect wetting as described in wetting theory, the polymer chains are free to diffuse into each other. The extent of inter-diffusion is highly dependent on the affinity of the two polymer surfaces and the extent of inter-diffusion is proportional to the Flory-Huggins interaction parameter between the two polymers. The Flory-Huggins interaction parameter, $\chi$, is related to the enthalpy of mixing of a polymer solute in a monomeric or polymeric solvent. The value of $\chi$ is dependent on the temperature, concentration, and molecular weight of the solute and solvent (Rosen, 1993). Compatible polymers can experience inter-diffusion of up to a few microns, while incompatible polymers are usually limited to inter-diffusion depths of only a few angstroms (Jabbari, Peppas 1994).

Further in their paper, Jabbari and Peppas continue to discuss polymer-polymer inter-diffusion and, in particular, molecular chain transport in polymer melts. According to the authors: "[In order to predict the] time dependence of chain interpenetration across a polymer-polymer interface, a mechanism of motion for the polymer chain [is needed]". Based on experimental observations they propose that reptation theory is the most accurate model, and that both overall mobility and the diffusion coefficient are proportional to $M^{-2}$ for a polymer chain (where M is molecular weight of a chain) (Jabbari, Peppas 1994). Generally speaking, according to reptation theory a polymer chain is only allowed to move within a

'tube' created by surrounding molecules thus limiting it from freely moving in three dimensions.

Fracture theory is less an adhesion theory and more a theory on how to determine adhesive forces by measuring fracture energy. The sum of the reversible and non-reversible works of adhesion, ε, can be determined by measuring fracture toughness, σ and using the equation below:

$$\sigma = \left( \frac{E\varepsilon}{\lambda_c} \right)^{1/2} \qquad \text{Equation 2.02.2}$$

where E is the Young's modulus of the polymer and $\lambda_c$ is the critical crack length. Fracture theory can also be used to determine the crack healing time of a polymer as it is related to the ratio of the fracture strength at a given time over the ultimate fracture strength of the polymer at infinite time (Jabbari, Peppas 1994). Due to the overall lack of chemical healing in polyethylene pipe, wetting and diffusion theory are expected to play a more significant roll in polyethylene adhesion than fracture theory.

Fujimatsu discusses the effects of using low density polyethylene (LDPE) gels as adhesives between HDPE plates (Fujimatsu, et.al. 1990). They acknowledge the generally poor adhesive properties of polyethylene, blaming its non-polarity and high crystallinity for this behavior. Based on their work however (Fujimatsu, Kuroiwa 1987, 1988), they have discovered that strong adhesive bonds can be created using HDPE and LDPE gels, using solvents such as tetralin, o-dichlorobenzene, and decalin. Their other papers cover, in detail, the experiments performed using HDPE gels, suggesting very high shear strengths of around 40 kg/cm$^3$ (~570 psi),

though the high temperatures required (110° C) result in softening of the moldings to be adhered. HDPE gels also displayed a wide range of solubility and shear strengths that was very dependent on the solvent used. To get around the problems discovered in HDPE gels, they moved on to using LDPE gels which required lower temperatures (70° C to 110° C), and displayed very little variability due to solvent choices (Fujimatsu, et al. 1990).

In order to create the LDPE gels they first had to purify the samples by dissolving the LDPE in purified xylene followed by precipitation and subsequent washing in cooled methanol. Once the LDPE was isolated, it was dried under reduced pressure at 60° C. Next they would prepare the gels by placing specified weights of purified LDPE in glass tubes with the chosen solvent. The LDPE was then dissolved completely at 140° C in an oil bath and then cooled until a gel was formed. The gels, once completed, were applied between two HDPE plates and heated for two hours. Afterwards they were allowed to sit at room temperature for 24 hours before testing (Fujimatsu, et. al. 1990).

Using these LDPE gels they were able to create bonds that had shear strengths ranging from below 5 kg/cm$^2$ at 70° C to nearly 30 kg/cm$^2$ (~430 psi) at 110° C. The LDPE gels resulted in lower observed shear strengths than the HDPE gels mentioned, but it was possible to form the gels at a much lower temperature than the HDPE (Fujimatsu, et al. 1990). Based on the results obtained by Fujimatsu et al. it seems that there is a very real possibility of using polyethylene gel technology in the development of a polyethylene pipe repair patch.

## 2.03 ANSYS: MODEL OF PE PATCH OVER CYLINDRICAL HOLE IN PIPE WALL

ANSYS 7.1 finite element modeling (FEM) software was used to model the stresses about a polyethylene patch covering cylindrical holes of various sizes on a section of polyethylene pipe. The goal of the model was to determine the primary mode of stress concentration about the patch (shear or normal) and use those results to establish success/failure criteria when testing the performance of selected adhesives.

The pipe and patch models were idealized as two, overlapping, 3-D partial cylinders assumed to be perfectly mated at the interface (see Figure 2.03.1); the lower piece will be referred to as the "pipe section", while the upper piece will be called the "patch section". The pipe section was then given a cylindrical hole normal to the curvature of the pipe, representing an idealized point of damage. Effects of the adhesive properties were neglected due to the difficulty of modeling and meshing the extremely thin adhesive layer (approximately 0.005 to 0.008 inches) in this model. The purpose of this model is not to predict when, or at what stress, the two layers will separate. Instead, the goal is to use the model to ascertain the maximum localized stresses that the patch will experience when the pipe is under any given internal pressure.

Figure 2.03.1: Pipe Cross Sections

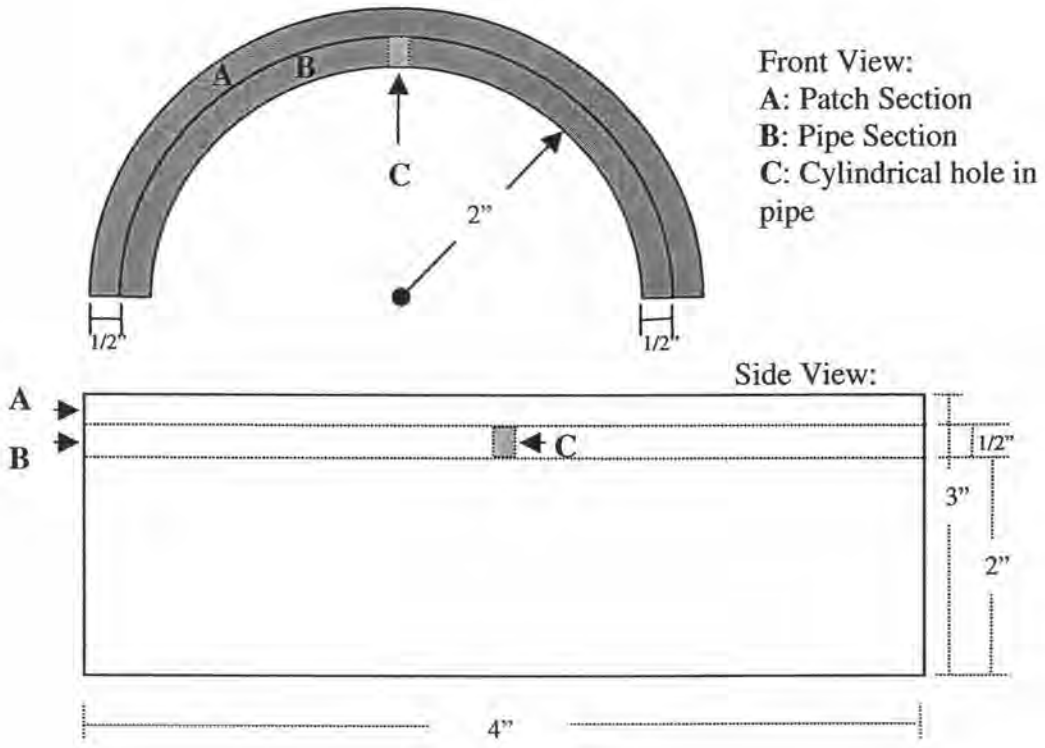


For this analysis, other types of damage beyond the idealized cylindrical hole were neglected; such investigations will become increasingly important as research continues because types of damage as well potential for damage propagation are, of course, important indicators of whether or not a patch will be sufficient for repairing the pipe. For now the goal is to simply gain an idea of the level of stress that the patch will experience for adhesive evaluation purposes.

The length of the section analyzed was 4-inches long on a 4-inch ID pipe of 0.5-inch wall thickness. The semi-cylindrical patch had an ID of 4.5-inches and a wall thickness of 0.5-inches; it was also 4-inches long. Two sizes of cylindrical

holes were applied to the pipe, one of 0.125-inch diameter and the other of 0.25-inch diameter; both were modeled at 2-inches in from each end at the center of the semi-cylindrical arc (90-degrees from horizontal). For each size of hole, two pressure loads were tested: one at 100-psi internal pressure and the other at 200 psi. The Young's Modulus for medium density polyethylene was determined to be 120,000 psi by analyzing stress-strain data gathered by Cheryl Carbone (See Appendix C). A Poisson ration of 0.3 was chosen (based on typical values for thermoplastic polymers [Hull, Clyne 1996]).

The pipe section and patch section were "glued" after the hole was placed in the pipe section, in effect causing them to behave as one continuous volume which was satisfactory for this model. Next, the volume was "meshed" into individual elements and nodes using the mesh tool interface. Initially a fairly large mesh was established using the auto-mesh option; the mesh sizing was then systematically reduced until there were between six and eight available elements on the inner surface of the modeled hole. When meshed, the elements were small and finely spaced near the hole and grew steadily larger as they moved further away. Finally, translational (i.e. motion) restrictions were placed on key points and surfaces of the volume and the pressure loads were applied (see Figure 2.03.2). See the ANSYS 7.1 help file for details on these functions.

Figure 2.03.2: Pipe Cross Section Translation Restrictions and Pressure Loads

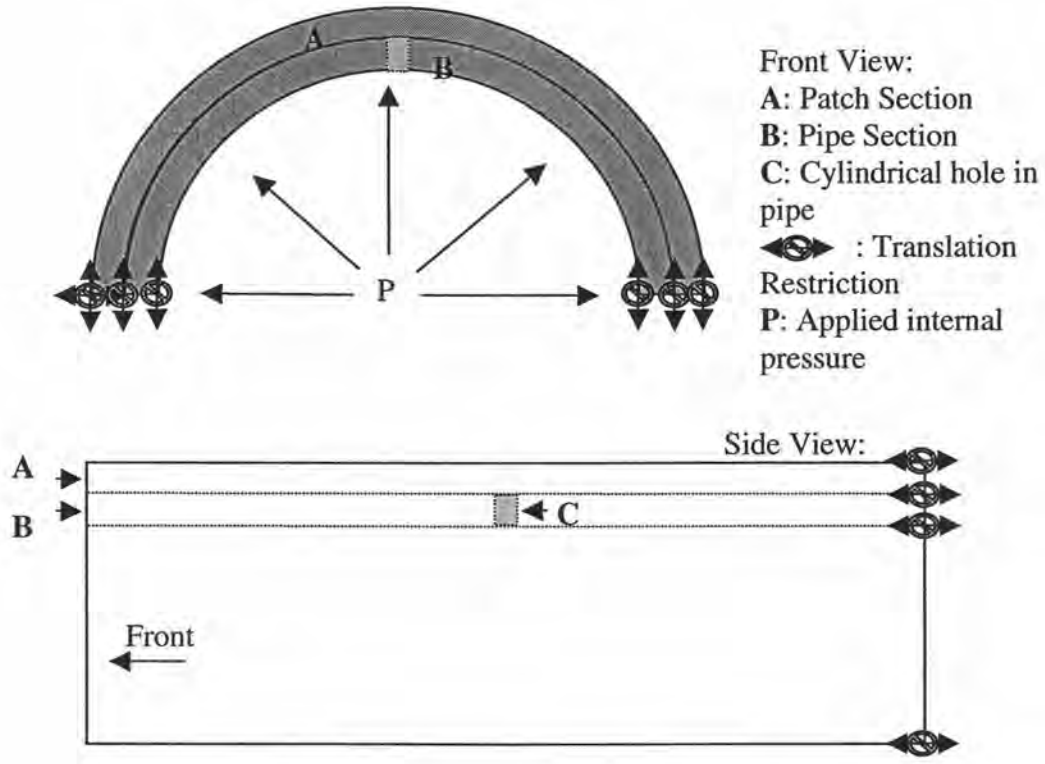


ANSYS was allowed to run its calculations and the model was analyzed. The results for these models are outlined below in Table 2.03.1.

Table 2.03.1: Stresses Experienced by Pipe Repair Patch

| Model | Normal Stress (psi) | Shear Stress (psi) |
|---|---|---|
| ½" thick patch over ⅛" diameter hole; 100 psi | 100 (average) | 413 – 530 |
| ½" thick patch over ⅛" diameter hole; 200 psi | 200 (average) | 826 – 1060 |
| ½" thick patch over ¼" diameter hole; 100 psi | 96 - 145 | 367 – 485 |
| ½" thick patch over ¼" diameter hole; 200 psi | 192 - 290 | 734 – 971 |

Due to expansion in the pressurized pipe, the greatest stress experienced by a patch will be in shear and within the same stress range as the hoop stress expected at the applied pressure (see hoop stress calculations in ASTM D 1598-02). Since most natural gas distribution pipes are operated at 50-60 psi and never over 100 psi (Brost, D. 10/2003), potential repair adhesives should be able to withstand at least 500 psi in shear to be considered for use in the pipe repair tool. Finally, the adhesive patch should be able to withstand a normal stress of 150psi.

## 2.04 EXPERIMENTAL

The strength of several adhesives in contact with high density polyethylene (HDPE) under a variety of environmental conditions were tested using shear tension loading as outlined in ASTM D 3165-95 [(ASTM D 3165-95)] with the exceptions to the method and sample preparation listed below. An Instron model TTBML was used for tension testing with an Instron 5000 kg load cell (model A216-11), and Instron Grips (model 2712-017). Data was collected using a Campbell Scientific 21X Data Logger.

Samples were cut from ¾ inch HDPE sheets into 5" by 1" sections as shown in Figure 2 of ASTM D 3165-95 [(ASTM D 3165-95)]. The 5" by 1" sections were then cut into 2" and 3" sections. The overlap used for the plastic sample pieces was 1", yielding final test pieces of 5" in length (see Figure 2.04.01), which is shorter than the 7" specimens described in ASTM D 3165-95 [(ASTM D 3165-95)]. This was done to reduce the influence of necking during the shear tension loading and to better fit between the grips used on the Instron. Before the samples were adhered, the 1" overlap area on each piece was carefully made by etching a shallow mark in the surface with the back of a sharp blade. The area to be bonded was then sanded with 240 grit paper using 16 strokes both perpendiculars to and with the length of the sample piece. This was done to ensure that the full 1-square inch section of overlap was completely and consistently sanded. The overlap section was then wiped off with 70% isopropyl alcohol solution to remove bits of plastic, dirt, and oil. Once the pieces were dry they were glued together, with the method of adhesive application dependent on the adhesive used; this will be covered shortly.

The adhered samples were then put under 7 to 10 pounds of direct pressure and subjected to varying cure times and environmental conditions prior to shear tension loading.

Figure 2.04.1: Test Specimen Configuration

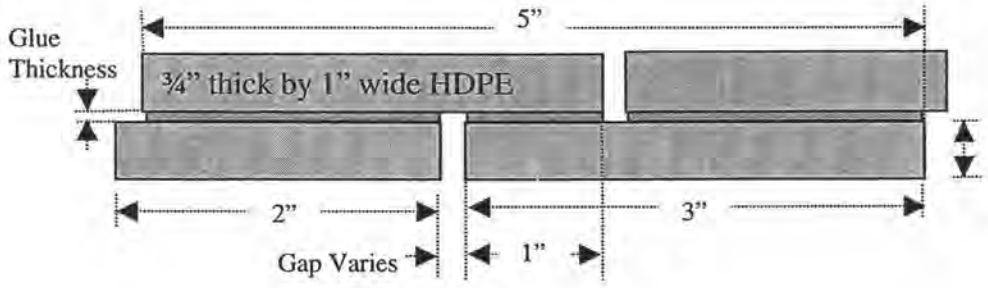


The adhesives used were 3M DP 8010, DP 8005 Translucent, and Phyllistran Socket Fast Blue. The 3M adhesives were designed for general use with polyethylene and a variety of other polymer surfaces with no surface pretreatment; they are all fairly viscous two part acrylic resins. The Socket Fast Blue was specifically designed for use with Phyllistran's polyethylene ropes used in the marine industry; it is a low viscosity two part adhesive.

The 3M two-part adhesives came with a specially designed glue gun to easily apply the 10:1 ratio of components, though it is possible to mix the components by hand. The two parts were mixed using a static mixer in the barrel of the glue gun. An even layer of adhesive was then placed on the 1 square inch sanded surface of one of the 3" pieces. The other 3" piece was placed with the sanded surface against the adhesive. Two 2" pieces were then attached, leaving about a ¼" gap between the glued sections (see Figure 2.04.01). Only the sanded overlap area is of interest for bonding properties; the 2" pieces are supplied to give

a good grip area for the instrument. Once the glue was applied, the samples were then placed under 7 to 10 pounds of pressure and allowed to cure before being exposed to environmental conditions and then shear tension loading. Once cured the thickness of the glue layer was measured and found to be, on average, 0.005 to 0.008 inches, which is the recommended thickness for the adhesive (Tech. Data Sheets, 3M DP 8005, DP 8010).

The Socket Fast Blue was applied in much the same way except that the two parts had to be mixed by hand and applied manually. Since the Socket Fast Blue was of significantly lower viscosity than the 3M adhesives the final thickness of the glue layers were typically less than 0.002 inches. Socket Fast Blue was designed to penetrate between the fibers in ropes, so no recommended glue thickness was provided (Tech. Data Sheet, Phyllistran Socketfast Blue).

The first set of conditions analyzed was generally referred to as "long term environmental experiments". In each case, a cure time of 15 hours at ambient temperature and humidity was met before exposing the adhesive to any other environmental conditions. 3M recommends 8 to 24 hours for full cure, while Phyllistran recommends 24 hours for Socketfast Blue under ambient conditions (Tech. Data Sheet, 3M DP 8005, DP 8010, Phyllistran Socketfast Blue). After the initial cure time was met the "long term samples" were then exposed to a variety of environmental conditions meant to simulate a patch under the ground. The four conditions analyzed were: dry-ambient (control), dry-cold, wet-ambient, and wet-cold. Dry-ambient samples were maintained at room temperature and ambient humidity for an additional 24 hours. Wet-ambient samples were placed in a tub of tap water at

room temperature for 24 hours. Dry-cold samples were placed in well sealed freezer bags and immersed in a bath of ice water which was kept under two degrees Celsius for 24 hours. Wet-cold samples were placed directly in a bath of ice water and kept under two degrees Celsius for 24 hours. At the time of testing, the samples were removed from the environment and immediately tested. Tests were performed as rapidly as possible due to an inability to maintain the environmental conditions during testing.

The second set of conditions analyzed was referred to as "short term elevated temperature experiments". These experiments were designed due to a curing note in the product literature suggesting that curing could be accelerated by heating the 3M DP8010 at 66-80 degrees Celsius for 30 minutes (Tech. Data Sheet, 3M DP8010). Samples were prepared as noted above in the "long term" experiments but were then tested in relatively short order. There were two general experiments run in the "short term" category: short-cure-ambient, and short-cure-high-temperature. The short-cure-ambient samples were prepared using only the 3M DP8010 adhesive and were prepared in the same way. However, once the samples were assembled, they were only allowed to cure for 30, 60, 90, and 120 minutes before testing. The short-cure-high temperature samples were also only made with 3M DP8010 adhesive and prepared in the same way, though once the samples were assembled two different experiments were attempted. In the first, the samples were allowed to cure in a programmable oven at 80 degrees Celsius for 30 minutes and were then allowed to cure for 30 and 60 minutes at room temperature before testing. In the second, the samples were allowed to cure with one side resting on a

hot plate set between 70 and 80 degrees Celsius for 30 minutes; they were then removed and allowed to cool and cure at room temperature for 40, 70, and 100 minutes before testing. The hot plate test was meant to simulate the effects of using a heated application tool which would only be able to supply heat to the outside of the patch surface. See section 2.05 for the experimental results.

## 2.05 EXPERIMENTAL RESULTS

Initial experiments were performed using the 3M adhesives (DP 8005 Translucent, and DP 8010) and Phyllistran Socketfast Blue at full cure times and under a variety of environmental conditions as outlined in section 2.04. The results for the experiments are outlined below.

Figure 2.05.1: Full Cure Times

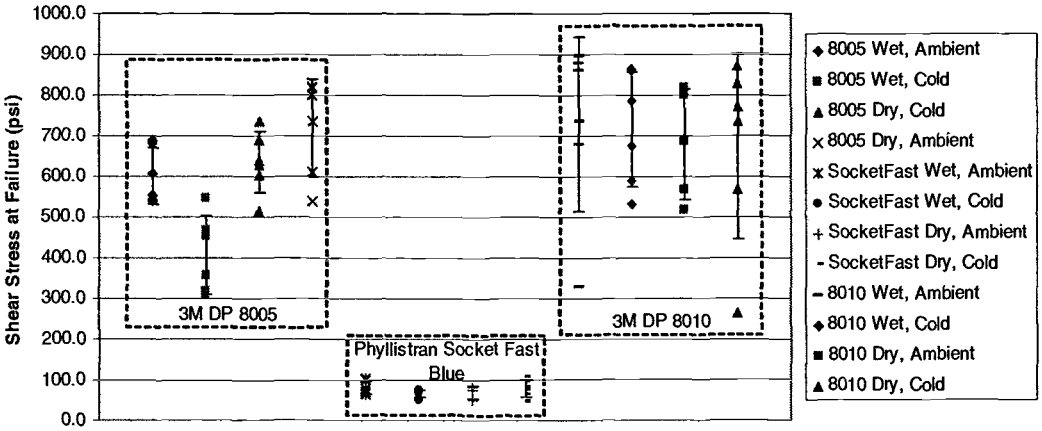


As seen in Table 2.05.1, the Socketfast Blue adhesive showed very low strengths in this application (≤100-psi), while the 3M glues all showed very high shear strengths over 500-psi with the exception of the 3M DP 8005 Translucent when immersed in an ice bath and the two outliers in the DP 8010 batch.

Based on these early tests, the Phyllistran and DP 8005 adhesives were dropped from the test matrix and experiments focusing on DP 8010 were performed. Due to the desired to keep labor times short during a pipe repair, short duration cure experiments at both ambient and elevated temperatures were

performed to see if structural bonds could be achieved in a relatively short period of time. The results of these experiments are shown below.

Figure 2.05.2: Short Cure Times

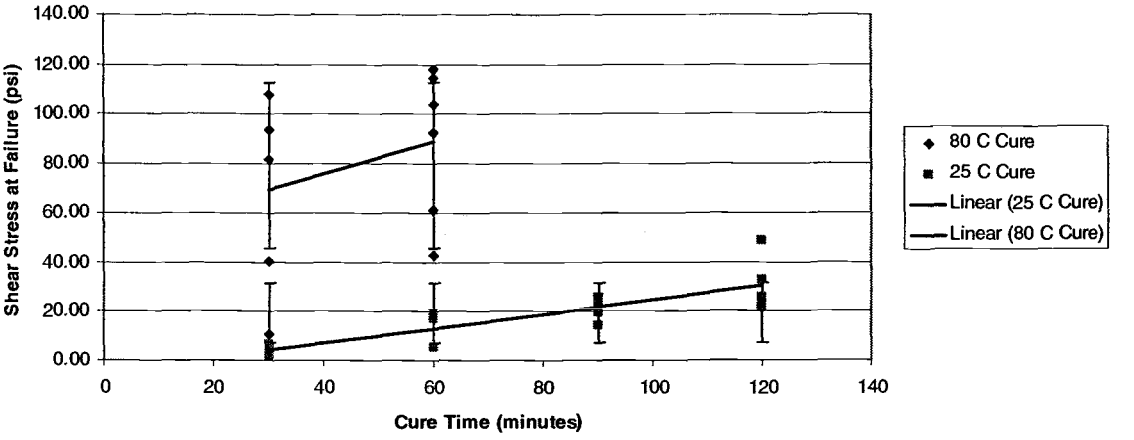


It is immediately clear that the increased cure temperature does increase the rate of curing, though it should still be noted that for all cure times examined the shear stress at failure did not exceed 120-psi. Also, the samples that underwent heated curing showed greater variability in the final strength than the samples allowed to cure under ambient conditions.

## 2.06 CONCLUSIONS

As stated in section 2.03, the expected shear stresses at the patch interface are between 370- and 530-psi for 1/8- and ¼-inch holes with 100-psi applied internal pressure. The normal operating pressures for the gas pipe lines are expected to be in the 60-psi range (Brost, D., 2003), a target shear strength of 530-psi was chosen as a goal for the adhesives used in the lap-shear tests to ensure that the adhesive would withstand normal operating pressure. Based on the full cure times for 3M DP 8005 and DP 8010, the ability to reach and exceed 500-psi is achieved, while the Socket Fast Blue is clearly unsuited for this particular application.

The problem that arises is not only one of final cure strength; also of concern is the time it takes for the adhesive to reach acceptable shear strength. For a patch to be considered acceptable, maintenance workers need to be able to excavate the damaged section of pipe, apply a repair patch and cover up the work area in a relatively short period of time. Ideally the patch would reach working adhesive strength in less than four hours considering that it takes four to six hours to excavate and replace a damaged section of pipe with current methods (Green, K., 2003). Based on the results obtained for the short duration cure times of 3M DP 8010, adequate shear strength is not achieved. 3M literature suggests strengths of 500 psi could be achieved within three hours (Tech. Data Sheet, 3M DP 8010); experiments performed in the lab did not achieve the two-hour strength of 100- to 200-psi given by the manufacturer ("Typical Rate of Strength Build-Up" (Tech. Data Sheet, 3M DP 8010)), though the short duration heated samples did come close. It should be noted that the literature states that the values listed in their tables are "considered

representative or typical only and should not be used for specification purposes." (Tech. Data Sheet, 3M DP 8010)

Obviously the limiting factor is not adhesive strength in the case of 3M DP 8010, but the time it takes for the adhesive to achieve a structural bond. To date, the DP 8010 and other adhesives examined fail to meet either the strength or time requirements (DP 8005, based on product literature, is not expected to make the cure time requirements needed) (Tech. Data Sheet, 3M DP 8005).

## 2.06.A FUTURE WORK

To date, an adhesive patch design that meets both strength and time requirements has yet to be found. In order to overcome this, one option includes expanding the study to include a wider variety of commercial adhesives. Another potentially more promising option would be to begin investigations into using polyethylene gels for the adhesive patch material. Based on existing literature, it seems that polyethylene gels may be able to meet the working strength requirements, possibly in shorter time scales than currently experienced with the commercial adhesives (Fujimatsu, et. al. 1987, 1988, 1990).

Also, expanding the ANSYS analysis to include non-idealized types of damage such as non-penetrating surface scratches and irregularly shaped gouges of various sizes would be insightful for further characterizing the types of damage that could potentially be successfully treated using an adhesive patch technology.

Finally, once a successful adhesive candidate was selected it would be necessary to damage and patch a section of polyethylene gas distribution pipe in the lab and measure its hydrostatic design basis once the adhesive had cured.

Ultimately, the adhesive patch will only be of use if the repaired pipe sections maintain their listed hydrostatic design basis after repair. The apparatus that would be used to test the hydrostatic design basis of polyethylene pipe is further discussed in chapter 3.

# 3.0 PIPE BURST TESTING

## 3.01 BACKGROUND

### 3.01.A PURPOSE OF RESEARCH

The second objective of this study was to develop a device capable of determining the hydrostatic design basis of polyethylene pipe specimens. This device will subsequently be called the "pipe burst tool" in this paper. The need for this tool is two-fold. First, Timberline Tool Company is developing a patented parallel-jaw pipe squeeze-off tool for 4 inch and 6 inch diameter polyethylene natural gas pipes. The development of this tool requires testing to ensure that the pipe squeeze-off tool does not compromise the hydrostatic design basis of polyethylene gas distribution pipe. Secondly, as the polyethylene adhesive patch project (described in chapter two) progresses, there will be a need to ensure that the patch performs correctly when applied to polyethylene pipe and is subjected to operating pressures.

The scope of this project is broken down into three general areas, the first of which is addressed in part in this writing.

After reviewing PPI TR-3/2003, ASTM D 2837-01, and ASTM D 1598-02 (see section 3.02) it became clear that the selection of the pipe end caps used in testing would be critical. Due to the high pressures used in validating the hydrostatic design basis of thermoplastic pipes, as well as the non-rigid nature of thermoplastic materials, it is critical to use an end cap design that will withstand the pressures used without slipping, destroying the pipe ends, or causing errors in the observed pipe failure mechanism. There are two primary choices in end cap

design: free and restrained end fittings (ASTM D 1598-02). Therefore, the first required step of this research requires analyzing and deciding on an end cap design to be used for subsequent pipe validation testing. Section 3.03 uses the ANSYS 7.01 program to model the effects of end cap design on the pipe hoop stresses in an effort to understand the end cap effects and make a choice for the final tool design. Next the end cap choices would be tested using sections of undamaged pipe, end caps, and a hydraulic hand pump to experimentally verify or discard the results from the ANSYS modeling, though this step is outside the scope of this writing.

The second step of this study would be to design and build the full scale pipe test apparatus using the selected end cap design. The design would be verified using undamaged pipe. The design and testing of the pipe test tool are, again, outside the scope of this work.

Finally the third step would be to use the completed pipe test apparatus to perform hydrostatic design basis validations on both crimped and adhesively patched pipes.

## 3.02 LITERATURE REVIEW

In order to design a pipe testing apparatus capable of confirming whether or not a pipe meets its hydrostatic design basis (HDB) three papers were used as guides in the design process. The first, TR-3/2003HDB/PDB/SDB/MRS Policies, is published by the Plastic Pipe Institute (PPI) and outlines the requirements for testing and validating pipe in accordance with the U.S. plastic pipe industry. The second, ASTM D 2837-01 Standard Test Method for Obtaining Hydrostatic Design Basis for Thermoplastic Pipe Materials, is referenced by TR-3/2003 and details the test methods needed for determining the HDB of plastic pipe and validating pipes of known HDB. The final paper, ASTM D1598-02 Standard Test Method for Time-to-Failure of Plastic Pipe Under constant Internal Pressure, covers the design and use of a test apparatus capable of performing the tests outlined in TR-3/2003 and ASTM D 2837. These three papers together provide the layout needed to determine the long term hydrostatic strength (LTHS) and, from that, the HDB for most thermoplastic materials, as well as methods for validating the HDB for existing thermoplastic pipe. Since the focus of this study is to determine whether or not crimped, and eventually repaired, pipe sections still meet their HDB, these methods will guide us to design an experiment and experimental apparatus capable of verifying the pipe performance.

"TR-3/2003 HDB/PDB/SDB/MRS Policies: Policies and Procedures for Developing Hydrostatic Design Basis (HDB), Pressure Design Basis (PDB), Strength Design Basis (SDB), and Minimum Required Strength (MRS) Ratings for Thermoplastic Piping Materials or Pipe" is a wide ranging paper which addresses

the plastic pipe industry's needs for procedures to determine the long-term strength ratings of thermoplastic piping materials and pipe. Much of the paper is not applicable to this study; however, the sections on grades of recommendations and data collection as well as the section dedicated to rating and validating polyethylene pipe are of utmost importance. Part A.2 covers the requirements for pipe grades at ambient and higher temperatures (23°C, 60°C, 82°C, and 93°C). In general, the pipe must meet specifications outlined in ASTM D 2837 for standard grades of pipe, as well as PPI requirements for experimental grades of pipes. For the purposes of this study, an analysis of standard grades of pipes that have undergone deformation from a pipe squeeze-off tool or been intentionally damaged and repaired with a patch will be performed. In addition to those outlined in part A, additional requirements specific to polyethylene pipe must be observed in part F which will be covered later. The remaining sections of part A are of little significance in this study, as are parts B, C, D, E, and G with the exception of part D.2 which outlines how to extrapolate the LTHS of a pipe at a given temperature assuming you know the LTHS of the pipe at a higher and lower temperature.

Part F covers specific policies, practices, and procedures for polyethylene piping materials and pipe. It includes sections on requirements for substituting thermal, UV, and other stabilizers into existing PE materials as well as developing new PE materials for use in piping. Section F.4 is of greatest interest as it lays the ground work for establishing a method to validate the HDB performance of polyethylene pipe. Care must be taken when using the term "validate". According to TR-3/2003, validation is "the process of ensuring that, for those

materials that exhibit a transition from ductile to brittle failure mode, this transition occurs after 100,000 hours at the rated temperature." Ductile failure is characterized by material deformation at the area of the break (stretching, necking, etc.). Brittle failure, however, does not have any visible (to the naked eye) signs of material deformation at the break. Section F.4.1.1 defines the methods needed to establish the HDB category for a pipe, which is not needed for this study, as the pipe to be validated already has an HDB rating. Section F.4.1.2 outlines how to validate a pipe for a given HDB by applying a stress to the pipe at elevated temperature and durations significantly shorter than those needed to initially establish the HDB. Tables F.4.1.1 and F.4.1.2 given in TR-3/2003 give the temperature, stress, and time requirements for validating 23°C and 60°C polyethylene pipe. Section F.4.3 gives the ISO 9080 method for validating elevated temperature HDB; however, since the HDB for pipe used in this study was determined at lower temperatures, this method will not be used and the validation method outlined in F.4.1.2 will be used exclusively. According to F.4.1.2, for the pipe to be validated at least six specimens must be tested at the temperature and stress values listed in the tables and the specimens must have a log average time to failure exceeding the value listed. If premature failure occurs, the stress levels at the temperature may be reduced by 15% as long as the minimum required time under load is increased by six times. The test specimens and method for applying load must conform to the method outlined in ASTM D 2837.

"ASTM D 2837-01 Standard Test Method for Obtaining Hydrostatic Design Basis for Thermoplastic Pipe Materials" is a test method designed to determine the

HDB for a thermoplastic material by first establishing its LTHS, as well as validating materials with a known HDB. To establish the LTHS for a thermoplastic material, it is subjected to a constant internal stress until a time at which the material experiences a rupture. Several data points are taken (ASTM D 1598) over a period of time not less than 10,000 hours and a log-log straight line regression of stress vs. time-to-rupture is developed and extrapolated to 100,000 hours. Non-failure that last longer than 10,000 hours may also be used, as long as they do not cause a decrease in the extrapolated LTHS. This extrapolation is considered acceptable as long as the data do not show excessive scatter or a pronounced "knee" in the plot. Should this occur then the requirements for the test method are not considered met and the data are classified as unsuitable for analysis. The stress at the extrapolated 100,000 hour point is considered the LTHS for that material at the temperature tested. The LTHS is then found on table 1 in ASTM D 2837 and the resulting HDB is read directly from there.

Though it is insightful to see how HDB are established, as mentioned before, it will not be part of this study. Instead section 5.7 in ASTM D 2837 will be used almost exclusively for the validation method. Assuming that the HDB for the pipe is known, use table F.4.1.1 in TR-3/2003 to determine the stress and temperature requirements for testing (TR-3/2003 requirements override ASTM D 2837 requirements when specifically regarding PE pipe materials). Test at least six specimens at the required stress level, they should then have a log average time-to-rupture greater than or equal to the time listed in the table to be considered for validation. According to note 10 in ASTM D 2837, "when an elevated temperature

HDB is validated by this standard method, all lower temperature HDBs are considered validated for that material."

"ASTM D 1598-02 Standard Test Method for Time-to-Failure of Plastic Pipe Under Constant Internal Pressure" covers the requirements for the experimental method and design of equipment used to measure the time-to-failure (rupture) of thermoplastic piping material and pipe. Using this method, pipes are subjected to a constant internal applied pressure under controlled environmental conditions until the pipe fails. Failure is defined as "any continuous loss of pressure with or without the transmission of the test fluid through the body of the specimen under test shall constitute failure." Failure can be due to ballooning, rupture, seepage, or weeping. The time to failure is then recorded as well as the applied pressure, which is used to calculate hoop stress on the walls of the pipe. The hoop stresses and time-to-failure data can then be used to determine the HDB for the pipe and perform validations as outlined in TR-3/2003 and ASTM D 2837 above.

The test apparatus design must have several features for accurate testing. A fluid bath to provide a constant temperature system for the test specimens with temperature tolerances within $\pm 2^{\circ}C$ must be included. A system for applying a constant pressure load to the inside of the pipe specimens over long periods of time must be used. Pressure may be applied to the specimens individually or through a manifold system as long as failure in one specimen does not result in the loss of pressure to the remaining specimens. A pressure gage and timing device must be available for each individual specimen so that the timing device measures the total

time that specimen is at 98% or more of the test pressure. The combined tolerance for the timing device and pressure gage shall not exceed ±2%. Either free or restrained end closures (caps) that can withstand the maximum applied pressure to the specimens may be used in the apparatus. Free end closures are to be used for referee tests for the PE thermoplastic pipe specimens. Free (unrestrained) end fittings are defined as: "a pipe specimen end closure that seals the end of the pipe against loss of internal fluid and pressure, and is fastened to the pipe specimen." A restrained end closure is "a pipe specimen end closure that seals the end of the specimen against loss of internal fluid and pressure, but is not fastened to the pipe specimen. Restrained end closures rely on tie-rod(s) through the pipe specimen or on external structure to resist internal pressure end thrust." According to note 4 in ASTM D 1598-02, due to the axial loading present in free end closures, the equivalent hoop stress in solid wall thermoplastic pipe is 11% lower than the hoop stresses for pipe with restrained end fittings at the same pressure. The relative merit of free and restrained end closures in this study will be fully discussed in section 3.03 and 3.04 of this paper.

The test specimens used will be cut so that the length between end fittings will be at least five times the average OD of the pipes. For 4-inch pipe and 6-inch pipe this will result in a test apparatus capable of supporting specimens of at least 30-inches in length. Prior to pressure loading, each specimen will be fully filled with the test fluid and allowed to condition until the test temperature is reached. The specimens will be supported in the test/conditioning chamber so that no bending occurs and in a way that does not use any circumferential support. Once

conditioned, pressure will be applied to the specimens until the test pressure is reached, at this point timing will begin and pressure held constant until failure occurs. The time to failure for each specimen will be recorded, not including any times of depleted pressure.

The hoop stresses which will be plotted against time to failure are calculated as follows:

$$S = \frac{P(D-t)}{2t} \qquad \text{Equation 3.02.1}$$

where:

S = hoop stress, psi

P = internal pressure, psi

D = measured average outside diameter, inches

t = measured minimum wall thickness, inches

Once the hoop stress and time-to-failure are obtained for each specimen, they are analyzed according to TR-3/2003 and ASTM D 2837-01 to obtain either the HDB or to validate the HDB for already rated thermoplastic pipe.

## 3.03 ANSYS: MODEL OF THE COMPARISON OF FREE VS. RESTRAINED END CAPS AND THEIR EFFECTS ON PIPE WALL STRESSES

ANSYS 7.1 finite element modeling software was used to model free end caps and restrained end caps and their effects on the body (hoop) stresses of a pipe section when subjected to constant internal pressure. This was inspired by ASTM D 1598-02, note 4 which states: "Free-end closures fasten to the specimen so that

internal pressure produces longitudinal tensile stress in additions to hoop. Compared to free end closure specimens, stresses in the wall of restrained-end closure specimens act in the hoop and radial directions only. Because of this difference in loading, the equivalent hoop stress in free-end closure specimens of solid wall thermoplastic pipe are approximately 11% lower than in restrained-end closure specimens tested at the same pressure. The test results for each specimen and the LTHS will reflect this difference in test method." Note that free-end closures are fastened directly to the end of the pipe specimens while restrained-end closures are held in place against internal pressure by a tie rod through the pipe or similar external means (ASTM D 1598-02).

Recall that ASTM D 1598-02 uses the following equation to calculate hoop stress:

$$S = \frac{P(D-t)}{2t} \qquad \text{Equation 3.03.1}$$

Where S is the hoop stress (psi), P is the internal pressure (psi), D the average outside diameter (inches), and t the minimum wall thickness (inches) (ASTM D 1598-02). This calculation, of course, does not take into account factors such as axial stresses, so it's understandable that the actual hoop stress may be different in a pipe with free-end closures when compared to actual natural gas pipe which could be considered semi-infinite at any given point, or when compared to specimens made with restrained end fittings. Free-end closures add axial stress to the body of the pipe specimen due to pressure on the end caps pushing the ends apart. The question is: would the actual hoop stress be lower with free-end closures than with restrained-end closures? ASTM D 1598-02, note 4, indicates that free end closures

should have lower equivalent hoop stresses than restrained end fittings. Intuitively, it would seem that, due to the additional axial stresses on the body of the pipe, free-end fittings would result in higher hoop stresses than restrained-end fittings. This runs contrary to the statement in note 4 of ASTM D 1598-02 and ultimately led to the decision to model the effects of end fittings on hoop stress.

The models used for this ANSYS comparison are based on 36-inch long, 4-inch internal diameter specimens of polyethylene pipe; the same dimensions that are to be used in the physical experiments. The models were created by making two dimensional axial cross sections of the pipe and using ANSYS 7.1 to extrapolate them into three dimensions using the "axisymetric" setting. In the free-end closure scenario, the end cap and body are considered one piece as seen in Figure 3.03.1; while for the restrained-end closure model, the end fittings are left off and the fittings are simulated by applying appropriate radial translational restraints on the outside ends of the pipe (Figure 3.03.2). The radial translational restraints in the restrained end cap scenario correspond to caps that overlap the ends of the pipe by two inches. There is nothing to constrain the end from "sliding" axially within the caps, thus eliminating any axial stresses on the body of the pipe. In both cases, axial translational constraints are applied to one point on the end of each pipe to prevent the model from "drifting" through space as a result of the simulation.

Figure 3.03.1: Free End Fitting

Approximate physical system: pipe with two caps welded on to ends.

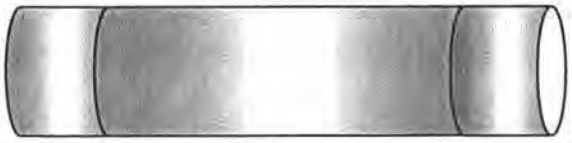

ANSYS model using axisymetric modeling. ◀▶ *indicates translation restriction.*

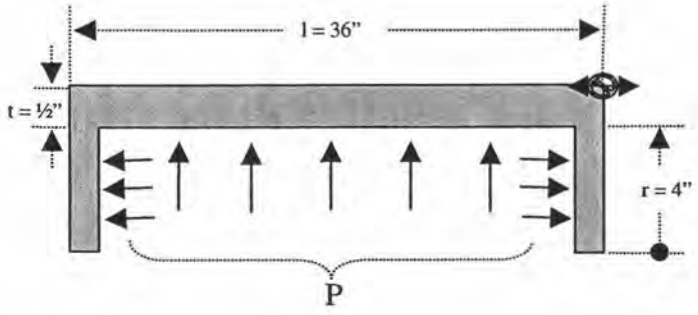


Figure 3.03.2: Restrained End Fitting

Approximate physical system: pipe with two caps and interior tie rod.

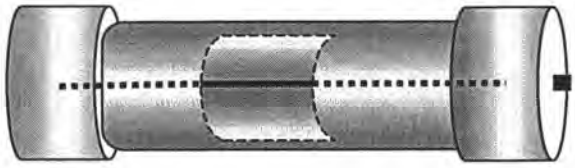

ANSYS model using axisymetric modeling. ◀▶ *indicates translation restriction.*

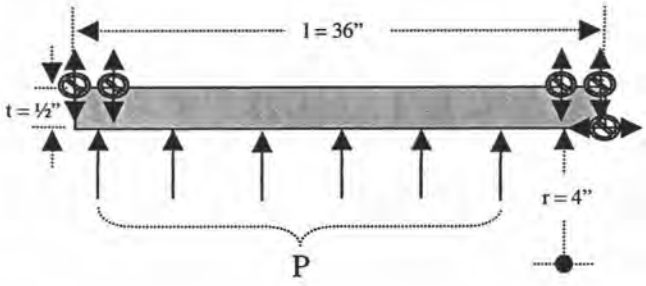

Both models were created using a modulus of 120,000-psi and a Poisson ratio of 0.3 (see section 2.4 for details). The internal pressure on the specimen models were varied from 100-psi to 400-psi and the results were compared with the hoop stress calculations given in ASTM D 1598-02. The results of the simulation are outlined below in Table 3.03.1.

Table 3.03.1: Free and Restrained End Cap ANSYS Model Results

| End Cap Type | Internal Pressure (psi) | Hoop Stress (psi) |
|---|---|---|
| Free End Fitting | 100 | 444 – 672 |
| | 200 | 888 – 1345 |
| | 300 | 1332 – 2017 |
| | 400 | 1776 – 2689 |
| Restrained End Fitting | 100 | 380 – 466 |
| | 200 | 760 – 933 |
| | 300 | 1141 – 1400 |
| | 400 | 1522 – 1867 |
| Restrained: ASTM calc. Equation 3.03.1 | 100 | 400 |
| | 200 | 800 |
| | 300 | 1200 |
| | 400 | 1600 |

From Table 3.03.1 the expected hoop stresses in pipes using a restrained end cap (for stress testing purposes) should have good agreement between the actual hoop stresses and the calculated hoop stresses (Equation 3.03.1). However, the experimentally *reported* hoop stresses (Equation 3.03.1), when using free end

fittings, will be lower than *actually* experienced by the pipe, as shown in table 3.03.1. In fact the actual hoop stresses when using free-end closures are expected to be higher than the restrained-end closures, contrary to the conclusions of note 4.

## 3.04 CONCLUSIONS AND FUTURE WORK

Based on the results of end-cap modeling using ANSYS 7.1, it seems that note 4 in ASTM D 1598-02 is, in part, wrong. The ANSYS results, however, are far from conclusive and further physical experimentation is required before denouncing the statement in note 4 [(ASTM D 1598-02)]. Future work will require that the two types of end fittings be compared against each other, using a statistically significant number of undamaged pipe specimens and comparing their relative burst pressures.

If the ANSYS modeling is correct, it should be observed that pipe specimens that have free end-fittings will tend to fail at lower pressure than those with restrained end-fittings. This would be due to the greater hoop stresses experienced in the free end-fitting specimens when compared to the restrained end-fitting specimens at any given applied pressure. If this turns out to be the case it would be advantageous to use restrained end fittings for two reasons. The first being that there is a very good correlation, based on modeling, between the observed (calculated) hoop stress and the suspected actual hoop stress in restrained end-fittings. The second reason would be for the additional security that a central tie rod would provide in keeping the end-fittings in place during experiments.

If, due to early experimental results, it is shown that the ANSYS model is wrong, then it would be necessary to go back and reevaluate the model until a good

correlation was found between observed (calculated) and suspected actual hoop stresses in the free and restrained end-fitting scenarios. The benefit of a good working model would be the confidence in hydrostatic design basis validation results gained knowing that a correct relationship between calculated and actual hoop stresses were observed.

Once an end-fitting design is chosen, the next step would be to design and test the full scale pipe tester. As mentioned in chapter 2.06, a finished test device would be used to establish whether or not an adhesive patch was capable of maintaining the hydrostatic design basis of a repaired pipe. It could also be used to test whether or not a section of pipe, once crimped using the tool designed by Timberline Tool Company, maintained its hydrostatic design basis as well.

# BIBLIOGRAPHY


1. 3M, (January 2003) "Scotch-Weld™, Structural Plastic Adhesive, DP-8005 Translucent – DP-8005 Black" Technical Data Sheet

2. 3M, (January, 2003) "Scotch-Weld™, Structural Plastic Adhesive, DP-8010" Technical Data Sheet

3. Allen, K. W. (November 1993), "Current theories of adhesion and their relevance to adhesive technology." *Journal de Physique* 3 no. 7 part 2, pp 1511-1516

4. ASTM D 1598-02, "Standard test method for time-to-failure of plastic pipe under constant internal pressure."

5. ASTM D 2837-01, "Standard test method for obtaining hydrostatic design basis for thermoplastic pipe materials."

6. ASTM D 3165-95, "Standard test method for strength properties of adhesives in shear by tension loading of single-lap-joint laminated assemblies."

7. Brewis, D. M., 1993, "Adhesion to Polymers: How Important are Weak Boundary Layers?" *Int. J. Adhesion and Adhesives* 13 no.4, pp 251-256

8. Brewis, D. M., Mathieson, I., Wolfensberger, M., (1995), "Treatment of Low Energy Surfaces for Adhesive Bonding." *Int. J. Adhesion and Adhesives* v15, pp 87-90

9. Brost, D., As cited in personal communication (October, 2003, Dan Brost of N.W. Natural Gas)

10. Chung, F. H. (1991), "Unified theory and guidelines on adhesion" Journal of Applied Polymer Science 42, pp 1319-1331

11. Fujimatsu, H., Kuroiwa, S. (1987), *Colloid and Polymer Science* 265, pp 747

12. Fujimatsu, H., Kuroiwa, S. (1988), *Colloid and Polymer Science*_123, pp 309

13. Fujimatsu, H., Ogasawara, S., Satoh, N., Komori, K., Matsunaga, Y., Kuroiwa, S. (1990), "Adhesive effect of low-density polyethylene gels on polyethylene moldings" *Colloid and Polymer Science* 268, pp 143-147

14. Green, K., As cited in personal communication (December 18, 2003, Ken Green of Timberline Tool)

15. Hess, R. (October 2003), As cited in personal communication (October 10, 2003, John Hunt, Timberline Tool and Reid Hess, Construction Training, Questar Gas Company, Salt Lake City, UT)

16. Hull, D., Clyne, T. W. (1996), An Introduction to Composite Materials 2nd edition, Cambridge University Press.

17. Jabbari, E., Peppas, N. A. (1994), "Polymer-polymer interdiffusion and adhesion." *J.M.S – Rev. Macromol. Chem. Phys.* C32(2), pp 205-241

18. Laramie, P. (Nov. 14, 2001) "Natural Gas Use to Increase 50 Percent in Next 20 Years, EIA Says" *American Gas Association*

19. Phillystran, Inc. "Socketfast Blue (A-20)", Technical Bulletin 109-6/97

20. Plastic Pipe Institute (2003), "Policies and Procedures for Developing Hydrostatic Design Basis (HDB), Pressure Design Basis (PDB), Strength Design Basis (SDB), and Minimum Required Strength (MRS) Ratings for Thermoplastic Piping Materials or Pipe" TR-3/2003 HDB/PDB/SDB/MRS Policies

21. Rosen, S. L. (1993), Fundamental Principles of Polymeric Materials 2nd edition, John Wiley and Sons, Inc.

22. United States. DOE/Office of Fossil Energy and NETL (September 2002), Natural Gas Infrastructure Reliability-Pathways for Enhanced Integrity Reliability and Deliverability

23. Watson, M. N., editor, (1998) *Joining Plastics in Production*, The Welding Institute.

# APPENDICES

# APPENDIX A: YIELD STRESS DATA

## Yield Stress Data for Figure 2.05.1: "Full Cure Times"

| H5TSWA | | H5TSWC | | H5TSDC | | H5TSDA | |
|---|---|---|---|---|---|---|---|
| Newtons | lbs | Newtons | lbs | Newtons | lbs | Newtons | lbs |
| 3038.9 | 683.2 | 2017.7 | 453.6 | 3264.8 | 734.0 | 3264.8 | 734.0 |
| 2402.2 | 540.0 | 1414.2 | 317.9 | 2796.7 | 628.7 | 2395.0 | 538.4 |
| 2466.6 | 554.5 | 1587.9 | 357.0 | 2687.2 | 604.1 | 3648.7 | 820.3 |
| 2409.0 | 541.6 | 2433.1 | 547.0 | 2836.5 | 637.7 | 3643.5 | 819.1 |
| 3063.0 | 688.6 | 2085.3 | 468.8 | 3069.8 | 690.1 | 3563.5 | 801.1 |
| 2694.1 | 605.7 | 1361.9 | 306.2 | 2283.5 | 513.4 | 2721.7 | 611.9 |
| avg | | avg | | avg | | avg | |
| 2658.2 | 597.6 | 1816.7 | 408.4 | 2823.1 | 634.7 | 3206.2 | 720.8 |
| stdev | | stdev | | stdev | | stdev | |
| 307.2 | 69.1 | 427.5 | 96.1 | 336.6 | 75.7 | 531.2 | 119.4 |

| P5TSWA | | P5TSWC | | P5TSDC | | P5TSDA | |
|---|---|---|---|---|---|---|---|
| Newtons | lbs | Newtons | lbs | Newtons | lbs | Newtons | lbs |
| 923.2 | 207.6 | 1020.6 | 229.4 | 1279.8 | 287.7 | 1253.7 | 281.8 |
| 678.0 | 152.4 | 483.2 | 108.6 | 937.1 | 210.7 | 1314.5 | 295.5 |
| 1043.2 | 234.5 | 999.7 | 224.7 | 1024.1 | 230.2 | 1882.1 | 423.1 |
| 985.8 | 221.6 | 999.7 | 224.7 | 1159.7 | 260.7 | 1579.4 | 355.1 |
| 1109.3 | 249.4 | 1189.3 | 267.4 | 86.6 | 19.5 | 1468.1 | 330.0 |
| 930.1 | 209.1 | 956.3 | 215.0 | 890.2 | 200.1 | 1690.7 | 380.1 |
| avg | | avg | | avg | | avg | |
| 944.9 | 212.4 | 941.5 | 211.7 | 896.2 | 201.5 | 1531.4 | 344.3 |
| stdev | | stdev | | stdev | | stdev | |
| 148.5 | 33.4 | 238.6 | 53.6 | 421.9 | 94.9 | 236.2 | 53.1 |

| HSFSWA | | HSFSWC | | HSFSDA | | HSFSDC | |
|---|---|---|---|---|---|---|---|
| Newtons | lbs | Newtons | lbs | Newtons | lbs | Newtons | lbs |
| 311.4 | 70.0 | 309.6 | 69.6 | 335.7 | 75.5 | 471.4 | 106.0 |
| 457.5 | 102.8 | 332.3 | 74.7 | 361.8 | 81.3 | 360.1 | 80.9 |
| 443.6 | 99.7 | 229.6 | 51.6 | 229.6 | 51.6 | 422.7 | 95.0 |
| 281.8 | 63.4 | 302.7 | 68.0 | | | 330.5 | 74.3 |
| 346.2 | 77.8 | 299.2 | 67.3 | | | 281.8 | 63.4 |
| 295.7 | 66.5 | | | | | 200.1 | 45.0 |
| avg | | avg | | avg | | avg | |
| 356.0 | 80.0 | 294.7 | 66.2 | 309.1 | 69.5 | 344.4 | 77.4 |
| stdev | | stdev | | stdev | | stdev | |
| 76.4 | 17.2 | 38.6 | 8.7 | 70.0 | 15.7 | 97.4 | 21.9 |

| H10SWA | | H10SWC | | H10SDA | | H10SDC | |
|---|---|---|---|---|---|---|---|
| Newtons | lbs | Newtons | lbs | Newtons | lbs | Newtons | lbs |
| 3013.9 | 677.6 | 3496.4 | 786.0 | 2525.7 | 567.8 | 3438.3 | 773.0 |
| 1467.7 | 330.0 | 2617.3 | 588.4 | 2303.0 | 517.7 | 3869.3 | 869.9 |
| 3911.1 | 879.3 | 3848.7 | 865.2 | 3048.7 | 685.4 | 1182.4 | 265.8 |
| 3271.3 | 735.4 | 2994.8 | 673.3 | 3643.5 | 819.1 | 3681.8 | 827.7 |
| 3981.1 | 895.0 | 3820.9 | 859.0 | 3563.5 | 801.1 | 2522.4 | 567.1 |
| 3834.8 | 862.1 | 2370.5 | 532.9 | | | 3273.9 | 736.0 |
| avg | | avg | | avg | | avg | |
| 3246.7 | 729.9 | 3191.4 | 717.5 | 3016.9 | 678.2 | 2994.7 | 673.2 |
| stdev | | stdev | | stdev | | stdev | |
| 953.5 | 214.4 | 626.7 | 140.9 | 600.7 | 135.0 | 1001.9 | 225.2 |

| P10SDA | | P10SDC | | P10SWA | | P10SWC | |
|---|---|---|---|---|---|---|---|
| Newtons | lbs | Newtons | lbs | Newtons | lbs | Newtons | lbs |
| 2114.2 | 475.3 | 2133.1 | 479.5 | 1467.1 | 329.8 | 1425.4 | 320.4 |
| 1853.2 | 416.6 | 1308.9 | 294.3 | 1477.5 | 332.2 | 1284.5 | 288.8 |
| 1808.0 | 406.5 | 1521.0 | 341.9 | 1569.8 | 352.9 | 1162.8 | 261.4 |
| 1856.7 | 417.4 | 1775.0 | 399.0 | 1771.6 | 398.3 | 1065.3 | 239.5 |
| 1879.4 | 422.5 | 1954.2 | 439.3 | 1754.2 | 394.4 | 1567.9 | 352.5 |
| 1976.9 | 444.4 | 1743.5 | 392.0 | 1545.4 | 347.4 | 1568 | 352.5 |
| avg | | avg | | avg | | avg | |
| 1914.7 | 430.5 | 1739.3 | 391.0 | 1597.6 | 359.2 | 1345.7 | 302.5 |
| stdev | | stdev | | stdev | | stdev | |
| 112.6 | 25.3 | 295.1 | 66.3 | 134.0 | 30.1 | 210.2 | 47.3 |

Yield Stress Data for Figure 2.05.2: "Short Cure Times"

25 °C Tests

| Run # | Time (min) | Max Stress (N) | Max Stress (psi) |
|---|---|---|---|
| 1 | 30 | 7.005 | 1.575 |
| 2 | 30 | 13.96 | 3.139 |
| 3 | 30 | 29.66 | 6.669 |
| avg | | 16.88 | 3.79 |
| sdev | | 11.61 | 2.61 |
| | | | |
| 1 | 60 | 76.62 | 17.23 |
| 2 | 60 | 24.45 | 5.495 |
| 3 | 60 | 85.32 | 19.18 |
| avg | | 62.13 | 13.97 |
| stdev | | 32.92 | 7.40 |
| | | | |
| 1 | 90 | 86.97 | 19.55 |
| 2 | 90 | 113.1 | 25.42 |
| 3 | 90 | 64.36 | 14.47 |
| 5 | 90 | 104.4 | 23.47 |
| avg | | 92.20 | 21.12 |
| stdev | | 21.50 | 5.84 |
| | | | |
| 1 | 120 | 146.2 | 32.86 |
| 2 | 120 | 215.7 | 48.50 |
| 3 | 120 | 113.1 | 25.43 |
| 4 | 120 | 111.4 | 25.03 |
| 5 | 120 | 95.75 | 21.53 |
| avg | | 136.42 | 24.00 |
| stdev | | 47.98 | 2.15 |

# APPENDIX B: INPUT VALUES FOR ANSYS MODELING

Chapter 2.03

Element: **SOLID187**
Global system / pure displacement
No USTRESS Routine

MAT Properties / MAT Modes:
- Structural
  - Linear
    - Elastic
      - Isotropic
        - **EX: 1.20E005** (Young's Modulus)
        - **PRXY: 0.3** (Poisson's Ratio)

Meshing:
- Mesh **Volumes**
- Shape: **Tet**
- **Free** Meshing (not mapped or sweep)
- Mesh Tool: **Smart Size 7**

Chapter 3.03

Element: **Plane 42**
- Parall to Global K1
- Include K2
- **Axisymetric** K3
- No extra output K4
- No extra output K5

Global system / pure displacement
No USTRESS Routine

MAT Properties / MAT Modes:
- Structural
  - Linear
    - Elastic
      - Isotropic
        - **EX: 1.20E005** (Young's Modulus)
        - **PRXY: 0.3** (Poisson's Ratio)

# APPENDIX C: DATA AND METHOD FOR DETERMINING YOUNG'S MODULUS

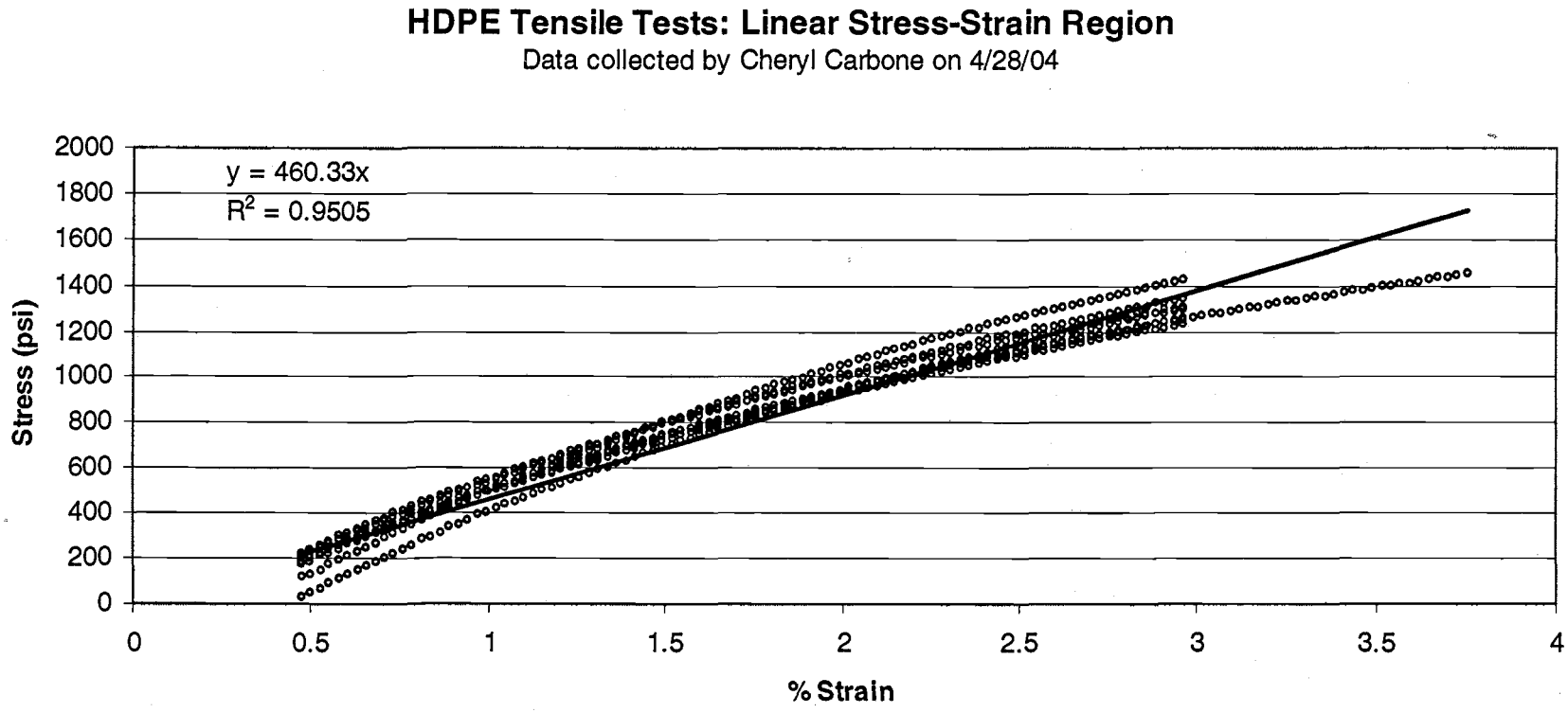

Calculation of Young's Modulus Based on Linear Stress-Strain Data

Based on information found in Ferry, J.D., 1970, Viscoelastic Properties of Polymers, the simple shear relaxation modulus (G) can be found by the following equation:

$G = \sigma_{21}/\gamma_{21}$

Where $\sigma_{21}$ is shear stress and $\gamma_{21}$ is shear strain.

By taking the slope of the linear best fit to the data presented above as the simple shear relaxation modulus

G = 460.33 psi/%

After converting the shear strain from a percentage to a decimal you get the following:

G = 460.33 psi/% (100%/1.0)

G = 46,033 psi

G ~ 46,000 psi

The Young's Relaxation Modulus, E, is related to G by the following equation according to Ferry on pg. 25:

$E(t) = 3G(t)$ or $E = 2G(1+\mu)$

$\mu$ is the Poisson ratio for the material (in this case 0.30). The Poisson ratio is a dimensionless number defined by the following equation which relates volume and tensile strain in a material:

$\mu = (1 - (1/V)(\delta V/\delta \varepsilon))/2$

Using these values the Young's Relaxation Modulus for the polyethylene samples tested is given by:

E = 2(46,000 psi)(1+0.30)

E = 119600 psi

E = 120,000 psi to two significant figures.